

Change from sixfold to fivefold coordination of silicate polyhedra: Insights from first-principles calculations of CaSi_2O_5

M. C. Warren and S. A. T. Redfern

Department of Earth Sciences, University of Cambridge, Downing Street, Cambridge CB2 3EQ, United Kingdom

R. Angel

Bayerisches Geoinstitut, Universität Bayreuth, D-95440 Bayreuth, Germany

(Received 4 June 1998)

Recent x-ray-diffraction observations found a triclinic phase of CaSi_2O_5 stable under ambient conditions, related to a monoclinic phase with the titanite structure. It differs from the titanite structure by the elongation and loss of a Si-O bond within a SiO_6 octahedron, thus having SiO_5 polyhedra. We have studied both these phases using density-functional theory in the generalized gradients approximation, to investigate the relative stability and chemical changes between the phases. Mulliken analysis is used to calculate covalent bond populations and atomic charges. A series of intermediate structures are studied to approximate a prototype transition pathway. [S0163-1829(99)06313-4]

I. INTRODUCTION

Silicon coordinated by five oxygen atoms is present as a component in aluminosilicate melts at the pressures and temperatures of the Earth's mantle, in which it dominates their transport properties.¹⁻⁸ Such SiO_5 groups are not normally found in silicate minerals, which contain SiO_4 tetrahedra at low pressures and an increasing proportion of SiO_6 octahedra at higher pressures. The recent determination of the room pressure structure of a phase of CaSi_2O_5 provided the first example of a crystalline oxide phase to contain silicon coordinated by five oxygens.⁹ Under a hydrostatic pressure of between 0.17 and 0.21 GPa this phase undergoes a first-order "displacive" phase transition to a monoclinic phase, during which the SiO_5 polyhedra become SiO_6 octahedra.¹⁰ The monoclinic phase was stable upon return to ambient pressure, indicating some hysteresis in the transition. This transformation in a crystalline structure, therefore, provides a model system in which the energetics of the formation of SiO_5 groups and the mechanism of transformation of such groups to SiO_6 octahedra can be determined.

The structure of the monoclinic, high-pressure phase of CaSi_2O_5 is of the titanite structure type. It contains SiO_6 octahedra which share corners to form chains of octahedra. These chains are cross linked by SiO_4 tetrahedra which also share corners with the octahedra and these together form a three-dimensional framework. The calcium atoms occupy the cavities within the framework. The transformation to the triclinic structure involves breaking one-eighth of the links between the tetrahedra and the octahedra, leaving the Si-O bonds intact within the tetrahedra, but producing an Si-O distance within the former octahedra that is too long (2.83 Å) to be considered bonded.¹⁰ The triclinic, low-pressure phase therefore contains chains of alternating SiO_6 octahedra and SiO_5 pentahedra, partially cross linked by SiO_4 tetrahedra.⁹

There has also been a theoretical prediction of SiO_5 pentahedra in a phase of silica (SiO_2),¹¹ formed from α quartz under the application of nonhydrostatic stress in molecular

dynamics simulations. At high pressures this phase was shown to be stable with respect to quartz, using density-functional theory (DFT) with the local-density approximation. In that study, the pentahedra decomposed to α quartz via intermediate fourfold coordinated polyhedra. The local geometry of the SiO_5 pentahedra was very similar to those found in CaSi_2O_5 , suggesting that these polyhedra may be found more generally than in only these two phases.

In this paper, we investigate both the monoclinic and triclinic phases of CaSi_2O_5 using first-principles electronic structure calculations, to further determine both the stability and the electron distribution of a phase with SiO_5 polyhedra. A plane-wave basis set is used to represent the electronic wave functions, so no assumptions are made about the bonding during the simulations. However, once the wave functions are obtained, they are analyzed using atomic orbitals and the Mulliken formalism, to assign charges and covalent bond populations.

II. FIRST-PRINCIPLES CALCULATIONS

The density-functional theory is used in the generalized gradients approximation (GGA) formulation of Perdew and Wang,¹² using the plane-wave total-energy code CETEP.^{13,14} Norm-conserving pseudopotentials generated using the Q_c tuning method^{15,16} represent the atomic nuclei and core electrons; in the case of Ca, ten valence electrons were required to obtain satisfactory behavior. Pseudopotentials enforce no assumptions about the coordination of an atom, so four-, five- and sixfold coordinated silicon atoms should all be treated equally. The Ca pseudopotential was generated with reference to a Ca^{2+} ion¹⁶ but those for Si and O use the neutral atom for *s* and *p* states, with standard ionized and excited reference states for *d* components. The silicon and oxygen pseudopotentials are those used in recent studies of

MgO (Ref. 17) and magnesium silicate perovskite¹⁸ in which they are described fully.

A basis set of plane waves with kinetic energy less than 1000 eV was used, giving convergence of the total energy to within 0.01 eV per atom, and a Pulay stress¹⁹ on the unit cell of $4 \text{ meV}/\text{\AA}^3$ or 0.6 GPa. The Pulay correction to the stress was estimated from fitting the total energies at five energy cutoffs from 980 to 1020 eV, and has an uncertainty of 0.2 GPa. However, the effect of this uncertainty is likely to be much less than systematic overestimation of the volume due to use of the GGA. Both of these uncertainties are therefore comparable to the experimental transition pressure, so these calculations may not be used to bound P_c more tightly. Improving the accuracy of the simulations in an attempt to better the experimental observations would require unfeasible amounts of computer time.

A unit cell containing four formula units was used for all calculations apart from the monoclinic structural optimization, since this allows direct comparison between the two phases. Four \mathbf{k} points in the full Brillouin zone were used, from the $2 \times 2 \times 2$ Monkhorst-Pack set.²⁰ Increasing the sampling to $4 \times 4 \times 2$ changed the energy by less than 1 meV per atom.

In order to determine whether there is an energy barrier to the transition between monoclinic and triclinic phases at zero pressure, the transition pathway is required. In principle this may be deduced as a path of minimum energy in the $3N + 6$ dimensional space formed by all coordinates, this is impractical from first principles. A simple path is thus assumed but may be tested to see whether it is close to the lowest energy route. Nine intermediate structures were generated by linear interpolation between the monoclinic and triclinic end points, of both the unit-cell vectors and the fractional positions, to give a prototype series of configurations to act as a transformation pathway.

Mulliken analysis

The bond strengths between Si-O pairs were previously deduced from the x-ray data by interpolation and extrapolation of empirical data.⁹ Here we analyze the electronic charge density calculated from first principles to obtain bond populations, using the method of Segall *et al.*^{21,22} in which wave functions with a plane-wave basis set are projected onto a set of atomic orbitals. We outline here the steps involved, since they are well described by the original authors.

In pseudopotential calculations, pseudo-orbitals of the valence electrons are generated during the production of the corresponding pseudopotential. These may be considered as a localized basis set, so that wave functions may be expressed as a linear combination of atomic orbitals. Outside the core region, the pseudo-orbitals replicate the true atomic orbitals, having a decaying magnitude, and are only truncated where their magnitude is negligible (having decayed to the order of 10^{-10}). They are not truncated by the use of a periodic supercell, because they are represented in reciprocal space using Bloch functions. The projection of wave functions represented in terms of a plane-wave basis set to a representation with localized orbitals has been developed and successfully applied elsewhere.²³ In that work, the incom-

pleteness of a localized basis set was expressed in terms of the ‘‘spilling parameter’’ \mathcal{S} , measuring how much of the plane-wave wave functions cannot be expressed using the localized orbitals.

The Mulliken charges and bond populations may be calculated using Mulliken analysis^{23,24} using the overlaps of the pseudo-orbitals. This has been demonstrated for zincblende semiconductors,²³ other simple bulk systems,²² and a TiO₂ grain boundary²⁵ in which a fivefold coordination was found similar to that discussed here. In this paper we demonstrate that the bond populations calculated using this method agree favorably with widely used empirical bond valence values.

The exact choice of orbitals has a significant effect on the values obtained, particularly on the absolute values of the charges^{21,22} but should have a much smaller effect on differences between corresponding charges in different phases. Using only s and p orbitals of Ca, Si, and O gave a spilling parameter $\mathcal{S} = 0.016$. Including the d orbitals for Si reduced \mathcal{S} to 0.010, and changed the absolute values of Mulliken charges and bond populations, but the resulting values gave much better agreement with empirically determined bond valence values, as described below. This larger basis set was used in all subsequent calculations. It gave positive bond populations from some Si to eight rather than six O, but the additional two interactions had very low values (0.01 compared to between 0.6 and 1.1 for Si-O within polyhedra) so this was taken as an indication of the uncertainty of the method. However, inspection of the differences in charges or bond populations between the two phases gave very similar values with or without inclusion of the Si d orbitals. Ca d orbitals were not considered; the pseudopotential used for Ca treats p and d orbitals with the same potential and very little d character is expected.

III. RESULTS

A. Structure and stability

The calculated equilibrium structures are shown in Tables I, II, and III. The decrease in volume from the triclinic to monoclinic phase, at zero pressure, was found to be 3.7%, compared to the experimental value of 2.9%. Volumes of both phases were up to 3% larger than experimental values: the GGA is known to often overestimate the volume.²⁶ The lattice parameters of the monoclinic phase are not uniformly larger than found experimentally: a is 2% smaller and c is 3.5% larger, reflecting the anisotropy within the structure. Bond lengths were generally within 1% of experimental values (average $l_{\text{calc}}/l_{\text{expt}} = 0.9989$, standard deviation 0.0067) for all except the broken Si...O distance in the triclinic phase (7.6% too long). However, nonbonded interactions are not expected to be so accurately determined.

The triclinic phase was found to be more stable at zero pressure and temperature, consistent with experimental observations, by 0.14 eV per formula unit.

B. Bonding

Interactions between Si and O generally show strong positive bond populations, as would be expected for bonds with significant covalent character. Their values are shown in Tables I and III. The greatest change between the monoclinic

TABLE I. Structural parameters of monoclinic phase compared with x-ray diffraction data of Angel *et al.* (Ref. 9) and bond populations from Mulliken analysis for Si-O within polyhedra.

	Expt.	Calc.	
a (Å)	6.543	6.415	(−2.0%)
b (Å)	8.392	8.459	(+0.8%)
c (Å)	6.342	6.568	(+3.5%)
β (°)	113.2	113.4	
Volume (Å ³)	320.1	327.1	(+2.2%)
Tetrahedra		Population	
Si-O-oct	1.629	1.621	1.05
Si-O-oct	1.631	1.627	0.98
Octahedra		Population	
Si-O-oct	1.709	1.710	0.89
Si-O-tet	1.825	1.823	0.61
Si-O-tet	1.862	1.889	0.58

and the triclinic structures is the large reduction in the bond population in the Si-O bond that was presumed broken on transformation of the SiO₆ octahedra to the SiO₅ pentahedra (see Fig. 1). In the latter, it is only 10% of the value of the bonded interaction within either the octahedra of the monoclinic phase, or the remaining Si-O bonds in the triclinic phase. The population in the broken bond is only a few times larger than that of the two extra positive Si-O bonding interactions in the octahedra, which were considered as showing the level of noise. By contrast, other bonds can be seen to increase in strength at the transition, such as that on the other side of the “bridging” tetrahedron to a full octahedron.

The changes in bond population are similar to those found in a TiO₅ structure found in a grain boundary in rutile,²⁵ in which an alternation of the bond order is found along Ti-O bonds near the five-coordinated Ti. In CaSi₂O₅, a similar effect may be observed in the bond population on progression around the ring shown in Fig. 2. The large population decrease in the “lost” Si^{VI/V}-O bond (denoted [5]...O-tet in Fig. 2) is accompanied by increases in the other bonds to O from this Si, especially to the diametrically opposite oxygen ([5]-O-tet) and, to a lesser extent, in the other bond in the

TABLE II. Cell parameters of triclinic phase compared with x-ray-diffraction data (Ref. 9) and equivalents in a doubled cell of the monoclinic phase.

	Triclinic		Monoclinic	
	Expt.	Calc.	Expt.	Calc.
a (Å)	9.206	9.215	9.317	9.383
b (Å)	7.550	7.623	7.358	7.388
c (Å)	9.288	9.393	9.317	9.383
α (°)	80.41	81.55	77.2	77.5
β (°)	125.6	125.4	126.5	126.4
γ (°)	135.6	134.9	137.3	137.0
Volume (Å ³)	329.9	339.5	320.1	327.1

TABLE III. Bond lengths and populations in triclinic CaSi₂O₅ compared with bond lengths in the monoclinic phase.

	Triclinic		Monoclinic		
	Expt.	Calc.	Population	Expt.	
Tetrahedron					
Si-O-oct	1.614	1.604	1.08	1.629	1.621
Si-O-[5]	1.639	1.637	0.90	1.629	1.621
Si-O-oct	1.636	1.628	1.01	1.631	1.627
Si-O-[5]	1.631	1.623	0.98	1.631	1.627
Bridging tetrahedron					
Si-O-oct	1.626	1.619	0.99	1.631	1.627
Si-O-oct	1.640	1.630	0.92	1.631	1.627
Si-O-oct	1.639	1.630	0.96	1.629	1.621
Si-O-	1.588	1.582	1.24	1.629	1.621
Octahedra					
Si-O-[5]	1.740	1.750	0.80	1.709	1.710
Si-O-tet	1.791	1.774	0.65	1.825	1.823
Si-O-tet	1.845	1.861	0.61	1.862	1.889
Si-O-[5]	1.756	1.771	0.78	1.709	1.710
Si-O-tet	1.855	1.877	0.57	1.825	1.823
Si-O-tet	1.787	1.775	0.68	1.862	1.889
Pentahedra					
Si-O-oct	1.670	1.662	0.97	1.709	1.710
Si-O-oct	1.681	1.681	0.96	1.709	1.710
Si-O-tet	1.697	1.676	0.79	1.862	1.889
Si-O-tet	1.782	1.776	0.68	1.825	1.823
Si-O-tet	1.825	1.834	0.60	1.825	1.823
Si...O	2.831	3.048	0.05	1.862	1.889

ring ([5]-O-bridge). This reduces the impact on the total bond population of the Si^{VI/V}. Around the “dangling” oxygen, the loss of one bond is partially compensated by population increase in the other bond, to the Si^{IV} in the ring (tet-O...[5]). This in turn affects the total bond population of the Si^{IV}, but the next Si^{IV}-O bond (tet-O-[5]) remains relatively constant; the Si^{IV}-O bonds outside the ring (to octahedra) decrease in population. Charge transfer is thus observed around this ring, and the net effects on the Mulliken charges are described in the next section.

The Si-O bond populations are compared in Fig. 3 to those calculated obtained with a widely used empirical scheme relating observed bond lengths to bond strengths through an exponential decay.^{27,28} Although the absolute value of the bond population in Mulliken analysis is strongly dependent on the exact set of atomic orbitals chosen²¹ it can be seen that including the Si *d* orbitals gives values which are closely clustered around the empirical values over the range of bond lengths for which the empirical relationship was derived. The empirical relationship is therefore within the mutual uncertainties of measurements and calculations, verified by this simulation. Note that inclusion of the sixth

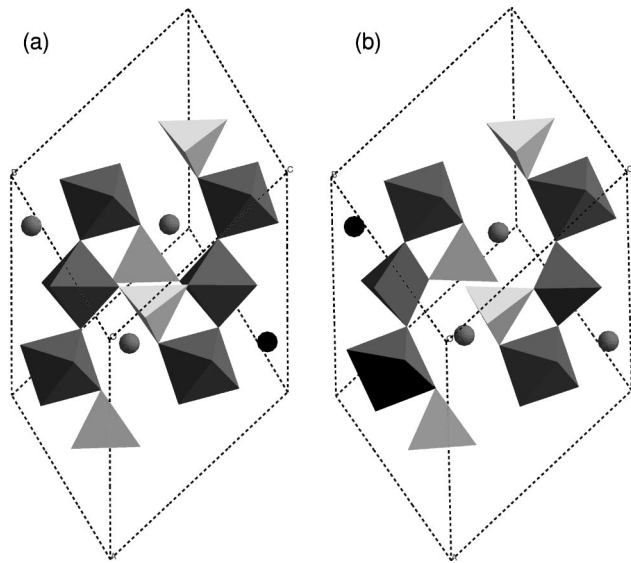


FIG. 1. Structures of (a) monoclinic and (b) triclinic CaSi_2O_5 , showing that a sixth oxygen has moved out of a SiO_6 octahedron to leave five-coordinated silicon.

Si-O distance from the SiO_5 group results in a slower decay of the exponential relationship, with an exponent of 2.14 compared to 2.70.

No positive bond populations were found between any Ca and O, but small negative values were found, indicating

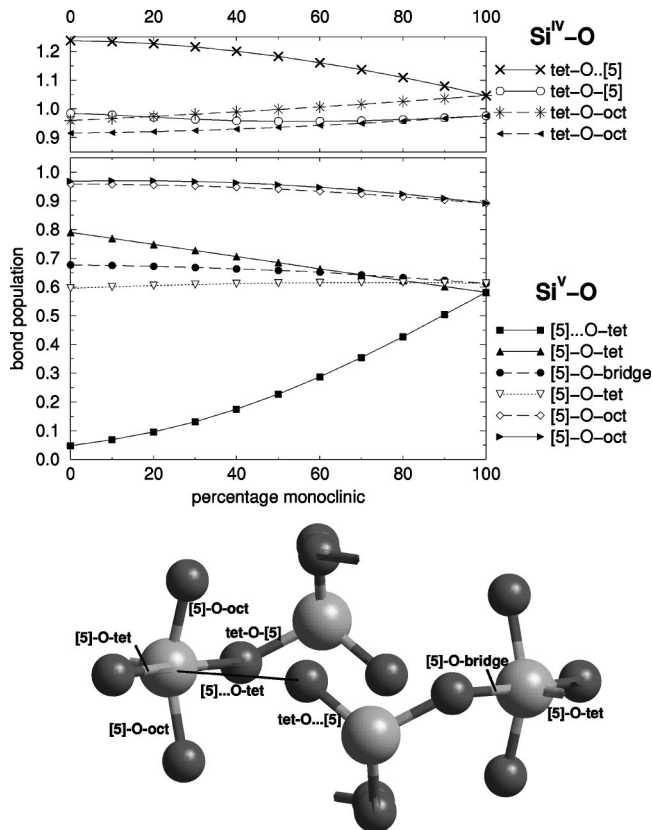


FIG. 2. Changes in bond population between the two phases, for selected Si-O bonds around the “lost” bond, and the structure fragment considered as a ring containing two tetrahedra and twofold, fivefold, or sixfold coordinated silicons.

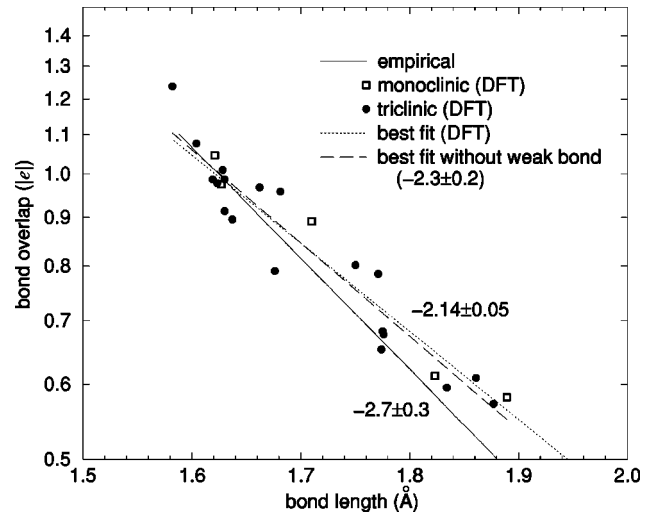


FIG. 3. Variation of bond valence (population) against bond length for the Mulliken calculations in monoclinic and triclinic phases and the empirical formula of Brese and O’Keefe (Ref. 28).

weak antibonding character. Purely Coulomb attraction is not, of course, included in these bond populations, but will also be present. The strength of the antibonding between the dangling oxygen and the two nearest Ca is comparable to the level of the “lost” Si-O bond in the triclinic phase. In the monoclinic phase there is a Ca-O antibond with population $-0.046|e|$, but in the triclinic phase this becomes $-0.061|e|$ and another Ca-O has population $-0.048|e|$. All other bond populations between this oxygen and other Ca ions are weaker than $-0.01|e|$.

C. Mulliken charges

The Mulliken charges associated with all atoms are also calculated. The absolute value of each charge is again strongly dependent on the basis orbitals used, but charge transfer during the transition may be reliably studied, as shown in Fig. 4. The charges on the oxygen atoms which lose a bond change by $-0.22|e|$, while the charges on all other oxygens change by less than $0.05|e|$. The charge increase on the silicon atoms is spread over not only the ^VSi ($0.05|e|$) but also the Si in the adjoining tetrahedra ($0.07|e|$) and octahedra ($0.08|e|$). The Si in the bridging tetrahedron gains $0.06|e|$ electrons, and so decreases in charge.

The variation between charges on nonequivalent Si and O is greater in the triclinic phase than in the monoclinic phase (standard deviation 0.049 compared to 0.033 for Si, and 0.070 compared to 0.035 for O), which is contrary to the expectation that more stable phases have more uniform charge distributions.¹⁰

IV. TRANSITION PATHWAY BETWEEN PHASES

The calculated energies of these phases are shown in Fig. 5. The energy curve suggests that there is an energy barrier

- ¹ *Structure, Dynamics and Properties of Silicate Melts*, edited by J.F. Stebbins, P. McMillan, and D.B. Dingwell, Reviews in Mineralogy (Mineralogical Society of America, Washington, D.C., 1995), Vol. 32.
- ² J.F. Stebbins and P. McMillan, *Am. Mineral.* **74**, 965 (1989).
- ³ X. Xue, J.F. Stebbins, M. Kanzaki, P.F. McMillan, and B. Poe, *Am. Mineral.* **76**, 8 (1991).
- ⁴ J.R. Rustad, D.A. Yuen, and F.J. Spera, *Phys. Rev. A* **42**, 2081 (1990).
- ⁵ C.A. Angell, P.A. Cheeseman, and S. Tamaddon, *Science* **218**, 885 (1982).
- ⁶ J.D. Kubicki and A.C. Lasaga, *Am. Mineral.* **73**, 941 (1988).
- ⁷ J.D. Kubicki and A.C. Lasaga, *Phys. Chem. Miner.* **17**, 661 (1991).
- ⁸ I. Farnan and J.F. Stebbins, *Science* **265**, 1206 (1994).
- ⁹ R.J. Angel, N.L. Ross, F. Seifert, and T.F. Fliervoet, *Nature (London)* **384**, 441 (1996).
- ¹⁰ R.J. Angel, *Am. Mineral.* **82**, 836 (1997).
- ¹¹ J. Badro, D.M. Teter, R.T. Downs, P. Gillet, R.J. Hemley, and J.L. Barrat, *Phys. Rev. B* **56**, 5797 (1997).
- ¹² J.P. Perdew and Y. Wang, *Phys. Rev. B* **45**, 13 244 (1991).
- ¹³ M.C. Payne, M.P. Teter, D.C. Allan, T.A. Arias, and J.D. Joannopoulos, *Rev. Mod. Phys.* **64**, 1045 (1992).
- ¹⁴ L.J. Clarke, I. Stich, and M.C. Payne, *Comput. Phys. Commun.* **72**, 14 (1992).
- ¹⁵ J.S. Lin, A. Qteish, M.C. Payne, and V. Heine, *Phys. Rev. B* **47**, 4174 (1993).
- ¹⁶ M.-H. Lee, Ph.D. thesis, University of Cambridge, 1995.
- ¹⁷ B.B. Karki, L. Stixrude, S.J. Clark, M.C. Warren, G.J. Ackland, and J. Crain, *Am. Mineral.* **82**, 51 (1997).
- ¹⁸ B.B. Karki, L. Stixrude, S.J. Clark, M.C. Warren, G.J. Ackland, and J. Crain, *Am. Mineral.* **82**, 635 (1997).
- ¹⁹ G.P. Francis and M.C. Payne, *J. Phys.: Condens. Matter* **2**, 4395 (1990).
- ²⁰ H.J. Monkhorst and J.D. Pack, *Phys. Rev. B* **13**, 5188 (1976).
- ²¹ M.D. Segall, C.J. Pickard, R. Shah, and M.C. Payne, *Mol. Phys.* **89**, 571 (1996).
- ²² M.D. Segall, R. Shah, C.J. Pickard, and M.C. Payne, *Phys. Rev. B* **54**, 16 317 (1996).
- ²³ D. Sanchez-Portal, E. Artacho, and J.M. Soler, *Solid State Commun.* **95**, 685 (1995).
- ²⁴ R.S. Mulliken, *J. Chem. Phys.* **23**, 1833 (1955).
- ²⁵ I. Dawson, P.D. Bristowe, M.-H. Lee, M.C. Payne, M.D. Segall, and J.A. White, *Phys. Rev. B* **54**, 13 727 (1996).
- ²⁶ G. Kresse, J. Furthmüller, and J. Hafner, *Phys. Rev. B* **50**, 13 181 (1994).
- ²⁷ I.D. Brown and D. Altermatt, *Acta Crystallogr., Sect. B: Struct. Sci.* **41**, 244 (1985).
- ²⁸ N.E. Brese and M. O'Keefe, *Acta Crystallogr., Sect. B: Struct. Sci.* **47**, 192 (1991).